

Video Article

Live-cell Measurement of Odorant Receptor Activation Using a Real-time cAMP Assay

Yuetian Zhang^{*1}, Yi Pan^{*1}, Hiroaki Matsunami^{2,3}, Hanyi Zhuang^{1,4}

¹Department of Pathophysiology, Key Laboratory of Cell Differentiation and Apoptosis of National Ministry of Education, Shanghai Jiao Tong University School of Medicine

²Department of Molecular Genetics and Microbiology, Duke University Medical Center

³Department of Neurobiology, Duke Institute for Brain Sciences, Duke University Medical Center

⁴Institute of Health Science, Chinese Academy of Science/Shanghai Jiao Tong University School of Medicine

* These authors contributed equally

Correspondence to: Yi Pan at lele1239@sina.com, Hanyi Zhuang at hanyizhuang@sjtu.edu.cn

URL: <https://www.jove.com/video/55831>

DOI: [doi:10.3791/55831](https://doi.org/10.3791/55831)

Keywords: Neurobiology, Issue 128, Real-time cAMP assay, odorant receptor, odorant, live-cell, kinetic measurement, muscone

Date Published: 10/2/2017

Citation: Zhang, Y., Pan, Y., Matsunami, H., Zhuang, H. Live-cell Measurement of Odorant Receptor Activation Using a Real-time cAMP Assay. *J. Vis. Exp.* (128), e55831, doi:10.3791/55831 (2017).

Abstract

The enormous sizes of the mammalian odorant receptor (OR) families present difficulties to find their cognate ligands among numerous volatile chemicals. To efficiently and accurately deorphanize ORs, we combine the use of a heterologous cell line to express mammalian ORs and a genetically modified biosensor plasmid to measure cAMP production downstream of OR activation in real time. This assay can be used to screen odorants against ORs and *vice versa*. Positive odorant-receptor interactions from the screens can be subsequently confirmed by testing against various odor concentrations, generating concentration-response curves. Here we used this method to perform a high-throughput screening of an odorous compound against a human OR library expressed in Hana3A cells and confirmed that the positively-responding receptor is the cognate receptor for the compound of interest. We found this high-throughput detection method to be efficient and reliable in assessing OR activation and our data provide an example of its potential use in OR functional studies.

Video Link

The video component of this article can be found at <https://www.jove.com/video/55831/>

Introduction

The sense of smell plays an important role in animals' survival as they rely on their olfactory abilities to obtain food, avoid predators and danger, distinguish species, and select mate^{1,2}. The realization of these functions depends on the odorant receptors (ORs), which are individually expressed at the ciliary surface of olfactory sensory neurons (OSNs) located in the olfactory epithelium (OE). ORs constitute the largest family of the G-protein coupled receptor (GPCR) superfamily with approximately 400 and 1200 diverse OR genes in human and mouse, respectively^{3,4,5}. ORs activated by odorants lead to increased intracellular cAMP levels via the sequential activation of olfactory G-protein (G_{olf}) and type III adenylyl cyclase (ACIII). The resulting increased level of intracellular cAMP could function as a second messenger, which opens the nucleotide-gated channel on the cell surface, triggering influx of cations including Ca^{2+} and action potentials, and ultimately initiating neuro-potential transmission and olfactory perception. The process of detecting and discriminating a large number of odorants by ORs is regarded as the first step of olfactory perception^{6,7}.

Since Buck and Axel⁸ first successfully cloned odorant receptors and elucidated the mechanism of olfactory perception initiated by ORs, deorphanization of the OR family became one of the hotspots in this field. Various *in vivo*, *ex vivo* and *in vitro* methods to measure OR activation have been reported^{9,10,11,12}. A traditional method that used Ca^{2+} imaging followed by single-cell RT-PCR on OSNs enabled the identification of different ORs to aliphatic odorants^{13,14,15}. More recently, the advent of large-scale transcriptome analyses promoted the development of more high-throughput *in vivo* methods. The Kentucky assay identified eugenol- and muscone-responsive mouse ORs with the use of the S100a5-tauGFP reporter mouse strain and microarray analysis⁹. Based on the decrease in OR mRNA levels after odorant exposure, the DREAM technology employed a transcriptomic approach to determine OR activation profiles in both vertebrate and non-vertebrate species¹⁶. Similarly, given the phosphorylation of S6 in neuronal activations, the Matsunami group sequenced mRNAs from phosphorylated ribosome immunoprecipitations to identify responsive ORs¹². Finally, the Feinstein group reported super sniffer mice that could serve as a platform to study odor coding *in vivo*, known as the MouSensor technology¹⁷.

In the *in vitro* realm, the challenge of culturing OSNs makes a heterologous expression system that mimics OR functional expression *in vivo* an ideal solution to conduct large-scale screening of odorous chemicals for ORs. Nevertheless, since cultured cell lines of non-olfactory origins differ from native OSNs, OR proteins are retained in the endoplasmic reticulum and unable to traffic to the plasma membrane, resulting in OR degradation and loss of receptor function^{18,19}. To solve this problem, extensive works have been made to replicate OR functional expression

on the cell membrane in heterologous cell lines. Krautwurst *et al.* first attached the first 20 amino acids of rhodopsin (Rho-tag) to the N-terminal of OR protein and this promoted the cell-surface expression of some ORs in human embryonic kidney (HEK) cells²⁰. By conducting a serial analysis of gene expression (SAGE) library analysis from single OSNs, Saito *et al.* first cloned the receptor-transporting protein (RTP) family members, RTP1 and RTP2, and the receptor expression enhancer protein 1 (REEP1) that facilitated OR trafficking to the cell membrane and enhanced odorant-mediated responses of ORs in HEK293T cells²¹. Based on these findings, the Matsunami group successfully established the Hana3A cell line, stably transfected with RTP1, RTP2, REEP1, and $G_{\alpha_{\text{off}}}$ in HEK293T, and transiently transfected with Rho-tagged ORs, for efficient OR functional expression. Subsequent studies revealed 1) a shorter form of RTP1, RTP1S, that could more robustly promote OR function than the original RTP1 protein and 2) the type 3 muscarinic acetylcholine receptor (M3R) that could enhance OR activity via inhibition of β -arrestin-2 recruitment, both of which were introduced to the heterologous expression system to optimize experimental output^{22,23}.

Several detection methods have been used to quantify receptor activation in heterologous systems. The secreted placental alkaline phosphatase (SEAP) assay works with a reporter enzyme transcriptionally regulated by cAMP response elements (CREs), making it an attractive option for assessing OR activation. The fluorescence is readily detected in a sample of the culture medium after the incubation with SEAP detection reagent²⁴. Using this method, the functions of ORs as well as a secondary class of chemosensory receptors expressed in the OE-the trace amine-associated receptors (TAARs) have been characterized^{25,26,27}. Another common method, the luciferase assay, uses a firefly luciferase reporter gene under the control of the cAMP response element (CRE). Measuring luminescence generated by luciferase production provides an efficient and robust means of quantifying OR activation^{10,11,28}.

Real-time cAMP assays have also been widely used in dynamically monitoring the function of heterologous or endogenous GPCRs. One example of such advanced assays takes advantage of a genetically encoded biosensor variant, which possesses a cAMP-binding domain fused to a mutant form of luciferase. When cAMP binds, the conformational change leads to the activation of luciferase, luminescence from which can then be measured with a chemiluminescence reader^{29,30}. The real-time cAMP technology has been reported suitable for the de-orphaning of human odorant receptors in HEK293 and NxG 108CC15 cells^{31,32,33}, as well as in the HEK293T-derived Hana3A cells^{34,35}. The Krautwurst group also described in detail the real-time cAMP technology to be suitable for bi-directional large-scale OR screening approaches^{32,33}.

Here we describe a protocol for measuring OR activation using a real-time cAMP assay in Hana3A cells. In this protocol, the luminescence of pre-equilibrated live cells is kinetically measured for 30 min following treatment with specific volatile compounds, representing a more efficient and accurate analysis of OR activation that are less susceptible to artifacts that occur in the cellular environment with prolonged time and odor-induced cell toxicities. This real-time measurement allows for a large-scale screening of both ORs and ligands, as well as characterization of specific OR-ligand pairs of interest. Using this method, we successfully identified OR5AN1 as the receptor for the musk compound muscone by performing a screening against 379 human ORs and subsequently confirming the positive screening result.

Protocol

1. Culturing and Maintenance of Hana3A Cells

1. Maintain cells in 10 mL of minimum essential medium (MEM) with 10% fetal bovine serum (FBS), 100 $\mu\text{g}/\text{mL}$ penicillin-streptomycin, and 1.25 $\mu\text{g}/\text{mL}$ amphotericin B in a 100-mm cell culture dish in a 37 °C cell culture incubator with 5% CO_2 . With every other passage, add 1 $\mu\text{g}/\text{mL}$ puromycin to maintain stable transfection of plasmids (See **Introduction**).
NOTE: Perform all steps involving cell culture in a class II biological safety cabinet to ensure sterile environment.
2. Subculture at a ratio of 10-20% in 100-mm dishes every 2-3 days.

2. Plating Cells for Transfection

1. Observe the Hana3A cells under a phase-contrast microscope to ensure cell viability and to estimate confluence.
2. Aspirate all medium from the cell culture dish.
3. Wash cells by adding 10 mL of phosphate-buffered saline (PBS) onto the plate, swirling the dish, and aspirating the PBS.
4. Add 3 mL of 0.05% trypsin-ethylene diamine tetraacetic acid (EDTA) onto the plate. Mix for 1 min or until all cells are afloat.
NOTE: Observe the progress of cells detaching from the bottom of the plate under the microscope as necessary.
5. Inactivate trypsin by adding 5 mL of MEM with 10% FBS and pipette up and down to break up chunks of cell mass.
NOTE: For plating prior to transfection, the medium used should not contain antibiotics. Addition of antibiotics may decrease transfection efficiency.
6. Transfer an appropriate amount of cells to a 15-mL tube depending on the number of plates to be transfected. For each 96-well plate, plate 2×10^6 cells, or approximately 1/5 of a 100% confluent 100 mm dish, giving a cell count of 2×10^4 cells per well or a density of approximately 15-30% confluence per well. Centrifuge tubes at 200 $\times g$ for 5 min and aspirate the supernatant without disturbing the cell pellet.
NOTE: Calculate the correct amount of cells to be plated onto 96-well plates to avoid overgrowing or undergrowing cells prior to stimulation.
7. Add an appropriate amount of MEM with 10% FBS into the 15-mL tube and pipette up and down to break up chunks of the cell mass. For each 96-well plate, resuspend the cells with 6 mL of MEM with 10% FBS.
NOTE: Be careful not to generate air bubbles in the tube.
8. Add the suspended cells into a reservoir. Using a multichannel pipette, pipette 50 μL of cells onto each well of a 96-well plate. Incubate overnight at 37 °C with 5% CO_2 .

3. Transfection of Plasmids

1. Prior to transfection, observe the plated cells to ensure a proper confluence of approximately 30-50% per well under a phase-contrast microscope and return to the incubator.

2. Prepare in advance the Rho-tagged OR construct^{11,21,22,28}, the accessory factor constructs (RTP1S^{22,36} and M3R²³), and the biosensor variant construct^{29,30} by miniprep. Quantify the DNA concentration by a spectrophotometer and adjust plasmid DNA concentrations (e.g., to 100 ng/μL) with distilled water as necessary.
3. **Preparation of the Transfection Mixtures**
 1. Prepare a plasmid transfection mixture in 500 μL of MEM for each 96-well plate according to **Table 1**.
NOTE: When different ORs are tested on the same 96-well plate, the volume of the transfection mixture and the amount of plasmid DNA added must be adapted in function of the number of transfected wells with a given OR.
 2. Prepare a transfection mixture in a tube with 18 μL of lipid-mediated transfection reagent in 500 μL of MEM.
4. Mix the plasmid mixture with the transfection mixture by pipetting up and down. Incubate at room temperature for 15 min.
5. Stop the reaction by adding 5 mL of MEM with 10% FBS.
6. Spread out a thick layer of sterile paper towels in the cell culture hood. Take a 96-well plate with cells from the incubator. Gently and repeatedly tap the plate upside-down on the pile of paper towel so that the medium is completely absorbed by the paper towel.
NOTE: Do not forcefully or abruptly tap the plate as one could lose cells.
7. Transfer 50 μL of the combined transfection mixture to each well of the 96-well plate and incubate overnight for 18-24 h at 37 °C with 5% CO₂.
NOTE: A time-managed transfection and stimulation schedule should precede the measurement when more than one 96-well plate are tested in one experiment in order to have all plates measured after the same transfection time and stimulus exposure time.

4. Stimulation and Measuring OR Activity Using the Real-Time cAMP Assay

1. Observe the transfected cells under a phase-contrast microscope to ensure a proper confluence of 50-80% per well and return to the incubator.
2. Prepare the stimulation medium by adding 10 mM hydroxyethyl piperazineethanesulfonic acid (HEPES) and 5 mM glucose to Hank's Balanced Salt Solution (HBSS).
3. Thaw the real-time cAMP assay substrate reagent aliquots on ice. Store substrate reagent at -80 °C at 55 μL per tube in PCR tubes. Use 1 tube per plate.
4. Prepare 2% equilibration solution by mixing 55 μL of the substrate reagent and 2750 μL HBSS/HEPES/glucose solution.
5. Spread out a thick layer of paper towels on the bench. Gently and repeatedly tap the plate upside-down on the paper towel so that the transfection medium is completely absorbed by the paper towel.
6. Wash the cells by pipetting 50 μL of HBSS/HEPES/glucose solution to each well.
7. Gently and repeatedly tap out the HBSS/HEPES/glucose solution from the 96-well plate.
8. Pipette 25 μL of 2% equilibration solution to each well and incubate at room temperature in dark for 2 h.
9. Prepare in advance 1 M odorant stock solutions in DMSO and store at -20 °C until used.
10. Prior to the end of the incubation time, dilute the odorant stock solutions to working concentrations in HBSS/HEPES/glucose stimulation medium.
NOTE: The concentrations of the odorant dilutions prepared in this step should be doubled to yield the correct final concentrations in each well.
11. Using a chemiluminescence plate reader and before odorant addition, measure the basal luminescence level of the plate for 2 consecutive times at a rate of 1000 ms per well³⁴.
12. Quickly remove the plate from the plate reader and add 25 μL odorant dilutions to each well and immediately start continuous luminescence measurement of all wells for 20 cycles within 30 min.
NOTE: Pipette carefully to avoid contaminating neighboring wells when using different odorants and/or different concentrations of the same odorants in the same plate.

5. Data Analysis

1. Export the data from the chemiluminescence plate reader software.
2. Calculate normalized OR response for each time point using the formula

$$(\text{luminescence}_N - \text{luminescence}_{\text{basal}}) / (\text{luminescence}_{\text{highest}} - \text{luminescence}_{\text{basal}})$$
 where N = luminescence value of a certain well; basal = average luminescence value of the two basal luminescence values; highest = highest luminescence value of a plate or a set of plates.
 NOTE: Depending on the purpose of the experiment, alternative graphical representations can be adopted. For example, for screening assays (see **Figure 1**) and for generating concentration-response curves, the luminescence value of a certain well at a desired time point during the kinetic measurement, such as the maximum value or the final value, can be used.

Representative Results

Muscone is the main aromatic component from natural musk. Recent studies identified OR5AN1 as a human receptor for muscone and other macrocyclic musk compounds based on homology to the mouse OR, MOR215-1, cloned from muscone-responsive glomeruli in behaving mice^{37,38}. By screening the human OR repertoire, our group and the Touhara group also identified OR5AN1 as a major receptor for two macrocyclic musk compounds, cyclopentadecanone and muscone, respectively, using the luciferase assay system^{38,39}.

Using the real-time cAMP assay described here, we screened the human OR repertoire against 30 μ M muscone (**Figure 1**). Among the 379 human ORs screened, OR5AN1 emerged with a prominent response to muscone, while the other ORs and the negative controls (the no-odor control and the empty vector control) did not show a significant response. The positive control tested OR5AN1 against 30 μ M musk tibetene, a ligand for OR5AN1 (unpublished data), and was used to normalize the ORs' response to muscone. For graphical representation of this set of data, we picked the time point when the maximum luminescence reading was achieved for OR5AN1 against 30 μ M musk tibetene.

We next examined the concentration-response relationship of the odor-OR pair with 3 different concentrations of muscone. For each concentration of muscone tested, during the first 20 min after muscone addition, the response by OR5AN1 gradually increased and then plateaued in the last 10 min (**Figure 2A**) while the trace for the no-odor addition control (0 μ M muscone) remained relatively flat. Higher concentrations of muscone evoked stronger OR responses than the lower ones, that is distinguishable throughout the measurement. Using the last time point from the kinetic measurement, we generated a concentration-response curve and the concentration for 50% of maximal effect (EC_{50}) value of the curve is estimated to be 20.82 μ M (**Figure 2B**).

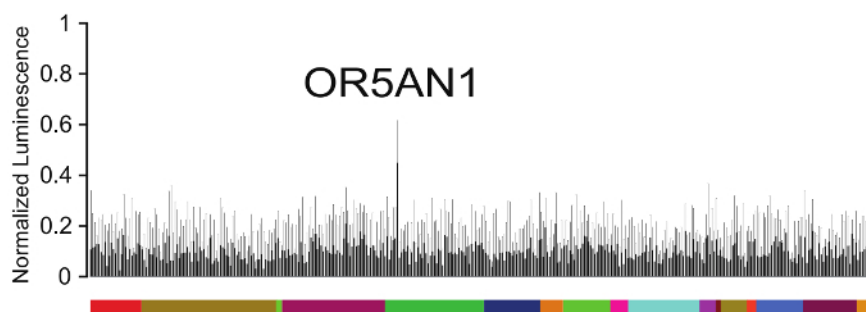


Figure 1: Screening for human ORs of muscone.

379 unique human ORs were screened against 30 μ M muscone using the real-time cAMP assay. Colored blocks along the x-axis indicate different human OR families. Every column on the x-axis represents a single OR type except for the last three columns, which are the response of OR5AN1 to 30 μ M musk tibetene (a positive control), the response of OR5AN1 to the HBSS/HEPES/glucose solution (a no-odor negative control), and the response of Rho-pCI to 30 μ M muscone (an empty vector negative control), from left to right. y-axis represents normalized luminescence at 30 min after odorant addition when the response reached a maximum for the positive control ($N = 3$). All responses are normalized to the positive control. Error bars represent standard error mean (SEM). For clarity, only positive error bars are shown. [Please click here to view a larger version of this figure.](#)

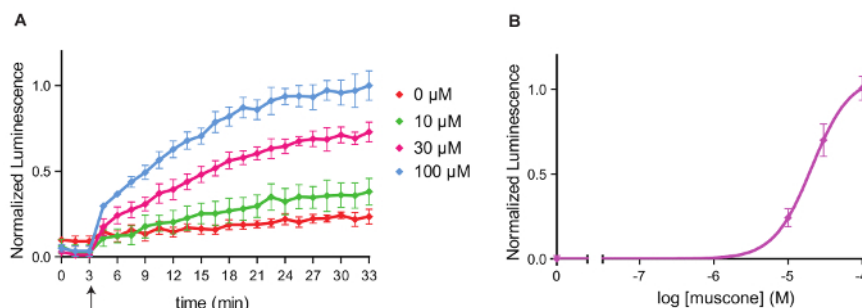


Figure 2: Kinetic measurements of the response of OR5AN1 to muscone.

(A) Real-time measurements of OR5AN1 activation by muscone of different concentrations and a no-odor negative control were performed within 30 min of odorant addition. Arrow indicates the time point of odorant addition. (B) Concentration-response curve of OR5AN1 against muscone at 30 min after odorant addition. y-axes represent normalized luminescence ($N = 3$). All responses are normalized to the highest response to 100 μ M muscone. Error bars represent SEM. [Please click here to view a larger version of this figure.](#)

Plasmid	Amount per 96-well plate (μ g)
Rho-OR	5
RTP1S	1
M3R	0.5
cAMP biosensor variant	1

Table 1: Components of the transfection mixture.

Per 96-well plate amount of the Rho-OR, RTP1S, M3R, and the real-time cAMP biosensor variant plasmids.

Discussion

Accurately measuring an OR's activation upon exposure to a certain odorant is the first step in deciphering the coding of olfactory information. The experiments shown in this study represent an example of how one can identify, using an *in vitro* OR expression system, responsive ORs among the human OR repertoire for the odorous chemical of interest and subsequently characterizing the receptor pharmacology using various

concentrations of the chemical. Our results confirm OR5AN1 as a *bona fide* receptor for muscone. This is consistent with a previous report³⁹ and provides further evidence for the speculation that only a small number of receptors are involved in sensing the musk odor^{27,40}. When compared with the screening data from Sato-Akuhara *et al.* that is generated by the luciferase assay on a similar OR heterologous expression system, our screening results showed slightly worse signal-to-noise ratio. Besides the variations inherent to the different techniques involved, the difference in the output could be due to the fact that we used a lower muscone concentration (30 μ M vs. 100 μ M). In fact, the EC₅₀ value of the concentration-response curve of OR5AN1 against muscone we obtained via the real-time cAMP assay is in the same order of magnitude as the one that Sato-Akuhara *et al.* obtained in their luciferase assay system, demonstrating comparable results for the same heterologous OR expression system even when different detection methods are used. In another study, our group found that the real-time cAMP system may be slightly more sensitive than the luciferase reporter gene system in assessing OR2T11 receptor selectivity, given that a small number of odorants were only active in the former but not in the latter system³⁵. When compared with the series of data reported by Geithe *et al.*³¹ on OR1A1 against (+)-carvone, our data on OR5AN1 against muscone showed a delay in the time needed to reach plateau, which might directly result from the different kinds of ORs and odorants used. In other real-time cAMP assay data reported from our group, we also showed varying times to peak depending on the ORs and odorants^{34,35}. In addition, different cell lines used to express ORs, different substrate used, different real-time cAMP biosensor variant plasmids, different sensitivity of the chemiluminescence plate reader, and/or different experimental conditions, such as variation in room temperature, could all contribute to the variations in luminescence output.

The real-time cAMP assay shows several advantages over other methods for measuring OR activation. First, similar to the luciferase reporter gene assay, the real-time cAMP assay provides an additional *in vitro* means of high-throughput identification of OR repertoires responding to odorants. Large-scale receptor and/or odorant screens by the real-time cAMP assay may offer a large amount of information on receptor-odor pairing with the use of a small number of plates. When advanced luminometers and pipetting robots are available, the 96-well protocol described here can be easily upgraded to a 384-well format, in which even less plasmid DNA and reagents are required per unit of data output. Second, the real-time cAMP method is capable of measuring changes in the intracellular concentration of cAMP in real time. While most assays used to measure OR activity to date are fluorescence- or chemiluminescence-based endpoint detection requiring cell lysis, the real-time cAMP assay is implemented under non-lytic, live-cell conditions that are more similar to the endogenous situation and that enable monitoring of changes in cAMP levels. Third, a relatively shorter time is required to perform the real-time method. Another high-throughput analysis method of OR function, which relies on a luciferase reporter gene expression, needs an additional 4 h after the odor stimulation to complete an experiment. In some cases, a prolonged odor incubation interval may result in potential odorant toxicity to cells, which is effectively alleviated under transient exposure. In addition, in longer-lasting experiments, the chances of contamination of neighboring wells by volatilization when using different odorants and/or different concentrations of the same odorant in the same plate are also increased. Immediate detection following odor addition makes the real-time cAMP assay a rapid and reliable paradigm.

The limitations of the real-time cAMP assay for measuring OR activation is as follows. First, our *in vitro* assay is based on a HEK293T-derived cell line which lacks many endogenous molecules of native olfactory sensory neurons. Furthermore, soluble proteins and enzymatic conversions occurring in the nasal mucus may bind with odorants and/or influence OR's affinity for odorants. Therefore, activation in the heterologous system may differ from the *in vivo* situation in terms of sensitivity and odor tuning. Second, the identification of ORs for a given odorant requires an entire OR repertoire of at least a given species. ORs are a large family of GPCRs and the numbers of OR proteins in human and mouse are very large^{4,5,41}. Considerable time and effort may be involved in cloning each OR repertoire of interest. Third, although the OR heterologous expression system includes OR sequence modifications (such as the Rho-tag) and some of the key OR accessory proteins (such as RTP1S and M3R), we suspect that not all ORs are functionally expressed on the cell membrane of the HEK293T-derived cells. Therefore, the absence of responses to a certain odorant *in vitro* does not necessarily preclude OR response *in vivo*, as a result of the fact that some ORs may just be poorly expressed on the cell surface and unable to recognize their ligands. Thus, whenever possible real-time cAMP should be used in conjunction with other *in vitro* and *in vivo* assays to obtain more convincing results.

Several critical steps should be given extra attention during the real-time cAMP assay. First, for experiments involving luminescence in general, temperature is a key factor that affects the result of the experiment as increases in temperature decrease basal and induced levels of light output and decreases in temperature increase light output. Therefore, pre-equilibrating the plates to the steady-state operating temperature of the instrument prior to odorant addition is necessary to avoid the influence on the results caused by temperature changes. Second, the concentrations of the real-time cAMP assay substrate reagent should be adjusted according to actual situation. When the basal luminescence fails to reach the lowest detection threshold of the chemiluminescence plate reader, one should consider increasing the substrate concentrations to increase signal. Finally, in spite of being an adherent cell line, Hana3A cells may detach during the experiment. When aspirating or adding the medium, placing the pipette tips at the side of the well can minimize disruption of the cell monolayer. It is also important to plate cells in an appropriate and uniform density to avoid overgrowing cells as dense spots of cells tend to peel off during the change of medium.

In addition to identifying OR(s) for an odorant of interest, the real-time cAMP assay can also be used to screen for cognate ligands for a given OR when libraries of chemicals are available. Finally, when appropriate cell types and transfection conditions are used, the assay may also allow for the detection of overexpressed or endogenous GPCR activation and give concentration-dependent response curves for both agonists and antagonists.

Disclosures

The authors have nothing to disclose.

Acknowledgements

The work was supported by the Chinese National Science Foundation (31070972), Science and Technology Commission of Shanghai Municipality (16ZR1418300), the Program for Innovative Research Team of Shanghai Municipal Education Commission, the Shanghai Eastern Scholar Program (J50201), and the National Basic Research Program of China (2012CB910401).

References

1. Malakoff, D. Following the scent of avian olfaction. *Science*. **286**, 704-705 (1999).
2. Zippel, H. P. The ecology of vertebrate olfaction D.M. Stoddart. Chapman and Hall, Andover, Great Britain, 1980. £15.00, 234 pp. ISBN 0-412-21820-8. *Behav Processes*. **7** (2), 198-199 (1982).
3. Dryer, L., & Berghard, A. Odorant receptors: a plethora of G-protein-coupled receptors. *Trends Pharmacol Sci*. **20**, 413-417 (1999).
4. Zhang, X., & Firestein, S. The olfactory receptor gene superfamily of the mouse. *Nat Neurosci*. **5**, 124-133 (2002).
5. Glusman, G., Yanai, I., Rubin, I., & Lancet, D. The complete human olfactory subgenome. *Genome Res*. **11**, 685-702 (2001).
6. Mombaerts, P. Genes and ligands for odorant, vomeronasal and taste receptors. *Nat Rev Neurosci*. **5**, 263-278 (2004).
7. Reed, R. R. After the holy grail: establishing a molecular basis for Mammalian olfaction. *Cell*. **116**, 329-336 (2004).
8. Buck, L., & Axel, R. A novel multigene family may encode odorant receptors: a molecular basis for odor recognition. *Cell*. **65**, 175-187 (1991).
9. McClintock, T. S. *et al.* In vivo identification of eugenol-responsive and muscone-responsive mouse odorant receptors. *J Neurosci*. **34**, 15669-15678 (2014).
10. Trimmer, C., Snyder, L. L., & Mainland, J. D. High-throughput analysis of mammalian olfactory receptors: measurement of receptor activation via luciferase activity. *J. Vis. Exp.* (88), e51640 (2014).
11. Saito, H., Chi, Q., Zhuang, H., Matsunami, H., & Mainland, J. D. Odor coding by a Mammalian receptor repertoire. *Sci Signal*. **2**, ra9 (2009).
12. Jiang, Y. *et al.* Molecular profiling of activated olfactory neurons identifies odorant receptors for odors in vivo. *Nat Neurosci*. **18**, 1446-1454 (2015).
13. Malnic, B., Hirono, J., Sato, T., & Buck, L. B. Combinatorial receptor codes for odors. *Cell*. **96**, 713-723 (1999).
14. Touhara, K. *et al.* Functional identification and reconstitution of an odorant receptor in single olfactory neurons. *Proc Natl Acad Sci U S A*. **96**, 4040-4045 (1999).
15. Kajiya, K. *et al.* Molecular bases of odor discrimination: Reconstitution of olfactory receptors that recognize overlapping sets of odorants. *J Neurosci*. **21**, 6018-6025 (2001).
16. von der Weid, B. *et al.* Large-scale transcriptional profiling of chemosensory neurons identifies receptor-ligand pairs in vivo. *Nat Neurosci*. **18**, 1455-1463 (2015).
17. D'Hulst, C. *et al.* MouSensor: A Versatile Genetic Platform to Create Super Sniffer Mice for Studying Human Odor Coding. *Cell Rep*. **16**, 1115-1125 (2016).
18. Lu, M., Echeverri, F., & Moyer, B. D. Endoplasmic reticulum retention, degradation, and aggregation of olfactory G-protein coupled receptors. *Traffic*. **4**, 416-433 (2003).
19. McClintock, T. S. *et al.* Functional expression of olfactory-adrenergic receptor chimeras and intracellular retention of heterologously expressed olfactory receptors. *Brain Res Mol Brain Res*. **48**, 270-278 (1997).
20. Krautwurst, D., Yau, K. W., & Reed, R. R. Identification of ligands for olfactory receptors by functional expression of a receptor library. *Cell*. **95**, 917-926 (1998).
21. Saito, H., Kubota, M., Roberts, R. W., Chi, Q., & Matsunami, H. RTP family members induce functional expression of mammalian odorant receptors. *Cell*. **119**, 679-691 (2004).
22. Zhuang, H., & Matsunami, H. Synergism of accessory factors in functional expression of mammalian odorant receptors. *J Biol Chem*. **282**, 15284-15293 (2007).
23. Li, Y. R., & Matsunami, H. Activation state of the M3 muscarinic acetylcholine receptor modulates mammalian odorant receptor signaling. *Sci Signal*. **4**, ra1 (2011).
24. Durocher, Y. *et al.* A reporter gene assay for high-throughput screening of G-protein-coupled receptors stably or transiently expressed in HEK293 EBNA cells grown in suspension culture. *Anal Biochem*. **284**, 316-326 (2000).
25. Liberles, S. D., & Buck, L. B. A second class of chemosensory receptors in the olfactory epithelium. *Nature*. **442**, 645-650 (2006).
26. Saraiva, L. R. *et al.* Combinatorial effects of odorants on mouse behavior. *Proc Natl Acad Sci U S A*. **113**, E3300-3306 (2016).
27. Nara, K., Saraiva, L. R., Ye, X., & Buck, L. B. A large-scale analysis of odor coding in the olfactory epithelium. *J Neurosci*. **31**, 9179-9191 (2011).
28. Zhuang, H., & Matsunami, H. Evaluating cell-surface expression and measuring activation of mammalian odorant receptors in heterologous cells. *Nat Protoc*. **3**, 1402-1413 (2008).
29. Fan, F. *et al.* Novel genetically encoded biosensors using firefly luciferase. *ACS Chem Biol*. **3**, 346-351 (2008).
30. Fan, B. F., & Wood, K. V. Live-Cell Luminescent Assays for GPCR Studies: Combination of Sensitive Detection and Real-Time Analysis Expands Applications. *Genetic Engineering & Biotechnology News*. **29**, 30-31, (2009).
31. Geithe, C., Andersen, G., Malki, A., & Krautwurst, D. A Butter Aroma Recombinate Activates Human Class-I Odorant Receptors. *J Agric Food Chem*. **63**, 9410-9420 (2015).
32. Noe, F. *et al.* OR2M3: A Highly Specific and Narrowly Tuned Human Odorant Receptor for the Sensitive Detection of Onion Key Food Odorant 3-Mercapto-2-methylpentan-1-ol. *Chem Senses*. (2016).
33. Geithe, C., Noe, F., Kreissl, J., & Krautwurst, D. The broadly tuned odorant receptor OR1A1 is highly selective for 3-methyl-2,4-nonanedione, a key food odorant in aged wines, tea, and other foods. *Chem Senses*. (2016).
34. Duan, X. *et al.* Crucial role of copper in detection of metal-coordinating odorants. *Proc Natl Acad Sci U S A*. **109**, 3492-3497 (2012).
35. Li, S. *et al.* Smelling Sulfur: Copper and Silver Regulate the Response of Human Odorant Receptor OR2T11 to Low-Molecular-Weight Thiols. *J Am Chem Soc*. (2016).
36. Wu, L., Pan, Y., Chen, G. Q., Matsunami, H., & Zhuang, H. Receptor-transporting protein 1 short (RTP1S) mediates translocation and activation of odorant receptors by acting through multiple steps. *J Biol Chem*. **287**, 22287-22294 (2012).
37. Shirasu, M. *et al.* Olfactory receptor and neural pathway responsible for highly selective sensing of musk odors. *Neuron*. **81**, 165-178 (2014).
38. Block, E. *et al.* Implausibility of the vibrational theory of olfaction. *Proc Natl Acad Sci U S A*. **112**, E2766-2774 (2015).
39. Sato-Akuhara, N. *et al.* Ligand Specificity and Evolution of Mammalian Musk Odor Receptors: Effect of Single Receptor Deletion on Odor Detection. *J Neurosci*. **36**, 4482-4491 (2016).
40. Gane, S. *et al.* Molecular vibration-sensing component in human olfaction. *PLoS One*. **8**, e55780 (2013).

41. Young, J. M. *et al.* Different evolutionary processes shaped the mouse and human olfactory receptor gene families. *Hum Mol Genet.* **11**, 535-546 (2002).